

Superconductivity above 130 K in the Hg-Pb-Ba-Ca-Cu-O system

Z. Iqbal

AlliedSignal Incorporated, Research and Technology, Morristown, New Jersey 07962

T. Datta, D. Kirven, and A. Lungu

Institute of Superconductivity, University of South Carolina, Columbia, South Carolina 29208

J. C. Barry

Centre for Microscopy and Microanalysis, University of Queensland Brisbane, Queensland 4072, Australia

F. J. Owens and A. G. Rinzler

*Armament Research, Development and Engineering Center, Picatinny, New Jersey 07806
and Hunter College, City University of New York, New York 10021*

D. Yang and F. Reidinger

AlliedSignal Incorporated, Research and Technology, Morristown, New Jersey 07962

(Received 18 October 1993; revised manuscript received 27 December 1993)

High volume fractions of the $n=2$ and $n=3$ members of a cuprate system of general formula $\text{Hg}_{1-x}\text{Pb}_x\text{Ba}_2\text{Ca}_{n-1}\text{Cu}_n\text{O}_{2n-2+\delta}$ (with an average value of x at 0.33) have been synthesized via a relatively facile process using low oxygen pressures. For as-synthesized $n=3$ (Hg,Pb-1:2:2:3) bulk superconducting critical temperatures (T_c) of up to 133 K have been observed. For $n=2$ (Hg,Pb-1:2:1:2), which is obtained with some rare-earth-ion substitution at the calcium site, T_c is 125 K after annealing in a reducing atmosphere. High-resolution lattice imaging coupled with structural simulations show that the Pb ions go into the Hg layer, leading to a chemical pressure-induced compositional modulation in this plane. Strong flux pinning and an irreversibility field of 1 T at 80 K are observed for Hg,Pb-1:2:2:3.

Superconductivity above 130 K was recently reported by Schilling *et al.*¹ and confirmed by Chu *et al.*² for samples prepared by a mercury-vapor transport process, in the $n=3$ (Hg-1:2:2:3) phase of the $\text{HgBa}_2\text{Ca}_{n-1}\text{Cu}_n\text{O}_{2n+2+\delta}$ system, shortly after the report of Putlin *et al.*³ of a transition temperature (T_c) at 94 K in $\text{HgBa}_2\text{CuO}_{4+\delta}$. In addition, it was observed that the T_c of the Hg-1:2:2:3 phase increases with pressure to above 150 K at 23 GPa.^{2,4} The pure $n=2$ phase (Hg-1:2:1:2) with T_c up to 128 K, and the Hg-1:2:2:3 phase have also been synthesized using high pressures to prevent the initial decomposition of HgO .^{5,6} Because of the absence of a trivalent element in these compounds, an excess of oxygen vacancies will be present, which is likely to make the Hg-based cuprates metastable, and hence inherently difficult to synthesize. We, therefore, replaced some of the Hg^{2+} ions with Pb^{2+} and Pb^{4+} ions in order to stabilize these structures, and allow their more facile and reproducible synthesis. In the present paper we describe such a reproducible synthetic route to large volume fractions of the $n=2$ and $n=3$ phases of the $\text{Hg}_{1-x}\text{Pb}_x\text{Ba}_2\text{Ca}_{n-1}\text{Cu}_n\text{O}_{2n+2+\delta}$ system, where the average value of x as determined by energy-dispersive spectroscopy is 0.33. The Hg,Pb cuprates are tetragonal with c -axis parameters that are similar to those of the Hg cuprates, indicating an absence of the "chemical pressure" expected due to the smaller Pb^{4+} ions in the lattice. However, a possibly stress-relieving compositional modulation is observed in high-resolution lattice images of the

Hg,Pb layer. An important result of the present study is the evidence of strong flux pinning in Hg,Pb-1:2:2:3, as shown for example by the observation of an irreversibility field $H^*(T)$, above 1 T at 77 K, where the current-carrying capacity of this type-II superconductor is lost. This value is significantly higher than that obtained for $\text{Bi}_2\text{Sr}_2\text{Ca}_2\text{Cu}_3\text{O}_{10}$ (Ref. 7) and $\text{HgBa}_2\text{CuO}_{4+\delta}$.^{8,9}

Our initial attempts to synthesize Hg-1:2:2:3 in sealed quartz tubes evacuated to 10^{-6} torr, and using the heat-treatment protocol reported by Schilling *et al.*,¹ produced nonsuperconducting samples that consisted primarily of BaCuO_2 , CuO , and CaHgO_2 . This suggested to us that Schilling *et al.*'s success in preparing these phases was due to possibly higher oxygen pressures in their reaction tubes, and their reported use of smaller amounts of Ca in their precursor composition. Extra oxygen can be introduced by incorporating an ion of similar size but higher valence (for example, Pb^{4+}) in the Hg plane, and by using higher oxygen partial pressures during synthesis. Based on these observations, we developed a two-step process which first involved the preparation of a precursor of a Ca-poor nominal composition $\text{Ba}_2\text{Ca}_{1.75}\text{Cu}_3\text{O}_7$. The precursor is synthesized from a stoichiometric mixture of nitrate powders, which is heated in flowing oxygen at 900°C for 16 h. The precursor is thoroughly mixed with carefully weighed quantities of HgO and PbO_2 . Under our synthesis conditions the most homogeneous samples were obtained using 0.8 moles of HgO and 0.2 moles of PbO_2 per mole of precursor. A pressed

pellet of the mixture is wrapped in gold foil and loaded in a quartz tube, which is pumped down to 10^{-6} torr, filled with 10^{-1} torr of pure oxygen, and then sealed. The quartz tube is placed inside a steel container and fired in a tube furnace using a protocol wherein the reaction temperature is raised to 800°C in 2–5 h, held at 800°C for 2 h and cooled to 30°C in 6 h. Relatively short firing times were used for the synthesis because the presence of lead was observed to catalyze the formation of the $n=3$ phase. Synthesis of pure Hg,Pb-1:2:1:2 is achieved by incorporation of more oxygen via substitution of the calcium ions with a trivalent rare-earth ion, such as yttrium.

The $\text{CuK}\alpha$ x-ray powder-diffraction (using a Rigaku diffractometer) data for the Y-doped Hg,Pb-1:2:1:2 and Hg,Pb-1:2:2:3 phases are shown in Fig. 1. The reflections corresponding to the $n=2$ and $n=3$ phases are indexed for a tetragonal cell with lattice parameters (calibrated using an internal standard) of $a=3.8612(8)$ Å and $c=12.640(4)$ Å, and $a=3.849(4)$ Å and $c=15.860(2)$ Å, respectively. In the Hg,Pb-1:2:1:2 phase sample, BaCuO_2 and CuO are present as impurities, while HgCaO_2 and CuO are observed as impurities

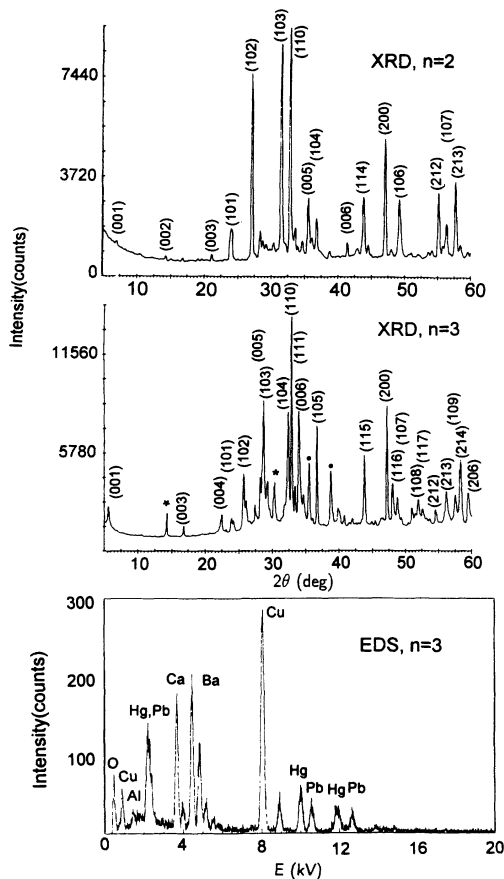


FIG. 1. X-ray diffraction (XRD) patterns for Hg,Pb-1:2:1:2 ($n=2$) and Hg,Pb-1:2:2:3 ($n=3$). The reflection indices are indicated. Reflections labeled (*) and (●) are associated with HgCaO_2 and CuO , respectively, in the diffraction pattern of the Hg,Pb-1:2:2:3 phase. The bottom trace shows the energy-dispersive spectrum (EDS) for a Hg,Pb-1:2:2:3 crystallite.

in Hg,Pb-1:2:2:3 . The values of the lattice constants are similar to those reported for the $n=2$ and $n=3$ phases of the Hg cuprate system,^{5,6} suggesting that effects of chemical pressure due to the incorporation of the smaller Pb^{4+} ions are minimal. The impurity phases were also detected using energy-dispersive spectroscopy (EDS) in a JEOL 4000FX electron microscope. The EDS data were collected using a Link detector and pulse processor, with a Moran Scientific analyzer. EDS data for the Hg,Pb-1:2:2:3 sample displayed in Fig. 1 show an average Hg:Pb ratio of 0.66:0.33 and an average composition of $(\text{Hg,Pb})\text{Ba}_2\text{Ca}_2\text{Cu}_3\text{O}_y$. Differences in the oxygen sublattice structure between the Hg and the Hg,Pb cuprates are indicated by Raman-scattering data on these materials. Samples of Hg,Pb-1:2:2:3 and $1:2:1:2$ show two intrinsic scattering peaks at 570 and 495 cm^{-1} , which can be assigned to the stretching vibration of the apical oxygen atoms coordinated respectively to the Hg^{2+} and the Pb^{2+} or Pb^{4+} ions in the mixed Hg,Pb-O layer. The presence of Pb^{4+} ions would also result in the presence of more intercalated oxygen in the Hg,Pb-O layer and a concomitant change in the apical-oxygen-bond force constant. By contrast the Raman spectra of Hg-1:2:2:3 and $1:2:1:2$ obtained by Ren *et al.*¹⁰ display a single apical-oxygen vibrational mode in the 580-cm^{-1} region, consistent with the presence of only Hg^{2+} ions in the Hg-O layer. Also, an increase in the apical-oxygen-mode frequency relative to that of the Hg,Pb-1:2:2:3 compound is observed, probably due to the presence of less intercalated oxygen in the Hg-O layer.

Lattice imaging at a structure resolution of 2.3 Å coupled with simulations were performed to determine the details of the structure of as-synthesized Hg,Pb-1:2:2:3 . A lattice image in the $[100]$ orientation taken at 400 kV is shown in Fig. 2. A simulation for defocus -800 Å, and thickness 12 Å, is shown as an inset in Fig. 2. In the simulation, which shows a good match to the $n=3$ phase, the Hg plane consists of 0.66 Hg and 0.33 Pb atoms. The atomic positions for the simulation were derived from the positions of the Hg-1:2:1:2 phase,⁵ to which extra Ca-O and Cu-O layers were added to model the three-layer compound. The Cu-O to Cu-O interplanar spacings were taken to be the same as that of the $n=3$ Tl-Pb-Sr-Ca-Cu-O compound.¹¹ The images show occasional intergrowths of the $n=2$ phase. Intergrowths of the four-copper-layer phase are also evident, albeit more rarely. The (100) electron-diffraction pattern (inset, Fig. 2) gives a c -axis spacing of 15.9 Å, in agreement with the x-ray-diffraction data. The electron-diffraction pattern shows intense diffuse scattering near the central beam, which extends over a reciprocal-space distance of 0.5 Å^{-1} from the center of the pattern (equivalent to a 2 -Å spacing in real space). We interpret the intense scattering to be due to vacancies in the oxygen sublattice, which are possibly induced by the compositional modulation in the Hg,Pb-O plane (see below). This observation suggests that the as-synthesized Hg,Pb-1:2:2:3 samples remain somewhat underdoped with respect to holes.

The lattice images display a modulation in the Hg,Pb layer, which is likely to be associated with a periodic Hg-Pb compositional variation. Note, however, that this

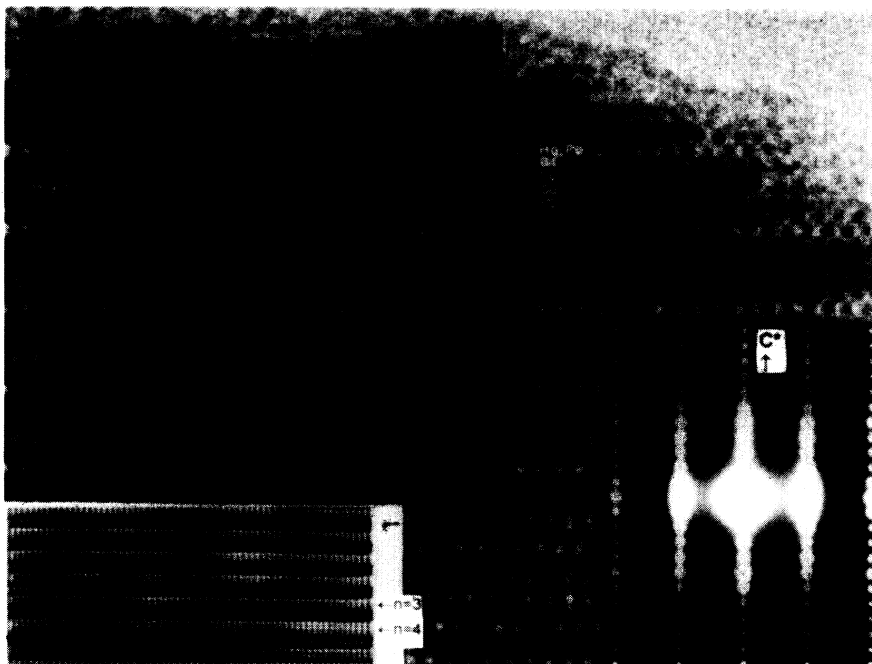


FIG. 2. [100] lattice image of a Hg,Pb-1:2:2:3 crystal. The inset at the top shows a lattice simulation. Simulation parameters are given in the text. Inset (bottom right) shows the corresponding electron-diffraction pattern, and inset (bottom left) shows a Fourier-processed (100) image.

modulation is not manifested as superlattice reflections in the electron-diffraction patterns. The Fourier-processed image (inset, Fig. 2) clearly shows that this somewhat irregular modulation extends to 30 \AA in the [110] direction. This modulation probably allows the lattice to relieve the chemical pressure induced by substitution of the smaller Pb^{4+} ions into the Hg,Pb plane, consistent with the observed absence of a decrease in unit-cell volume in the Hg,Pb cuprates relative to the pure Hg cuprates. The compositional modulation and defects induced by it in the oxygen sublattice may provide the key doping and flux-pinning centers in the Hg,Pb cuprates.

Figure 3 shows the normalized dc resistivity data ob-

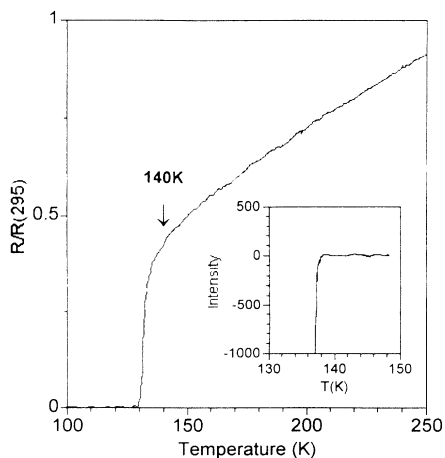


FIG. 3. Normalized four-probe dc resistivity versus temperature for a typical Hg,Pb-1:2:2:3 specimen. The inset shows the temperature dependence of the low-field (100 G) modulated microwave absorption intensity for a Hg,Pb-1:2:2:3 sample measured at a modulation field of 10 G.

tained in the four-probe configuration for a typical as-synthesized Hg,Pb-1:2:2:3 sample. Zero resistance occurs at a temperature of 130 K, while the transition onset temperature is near 140 K. Superconducting quantum interference device (SQUID) (SHE VTS 900) magnetometer data in a 50 G field for this sample, shown in Fig. 4, indicate a single diamagnetic transition with an onset temperature of 133 K, and a zero-field-cooled (ZFC) superconducting volume fraction greater than 80%. However, the field-cooled (FC) volume fraction is a factor of 10 lower, most likely due to a high degree of flux pinning in the sample. This conjecture is supported by SQUID (Quantum Design) magnetization measurements at 1G on a similarly synthesized but powdered Hg,Pb-1:2:2:3 sample with a diamagnetic transition onset at 132 K, where the FC susceptibility after diamagnetic corrections is 50% of $-1/4\pi$ at 100 K, and the ZFC volume fraction is over

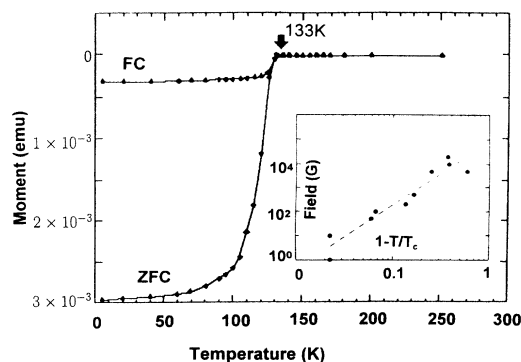


FIG. 4. 50-G field-cooled (FC) and zero-field-cooled (ZFC) magnetization data for a Hg,Pb-1:2:2:3 sample. The inset shows a plot of the irreversibility field versus the reduced temperature for two Hg,Pb-1:2:2:3 samples.

90%. Careful measurements of the onset temperature of modulated low-field microwave absorption, which is caused by flux jumps across local Josephson junctions formed in the superconducting state, have been made on a number of Hg,Pb-1:2:2:3 samples using an electron paramagnetic resonance spectrometer (Varian E9) operating at 9.2 GHz. These measurements indicate an onset T_c of 138 K as can be seen from the temperature-dependent data for a Hg,Pb-1:2:2:3 sample shown in Fig. 3 (inset). This temperature is near the resistive onset temperatures for similar samples (Fig. 3) but it is about 5 K higher than the values obtained from SQUID magnetometer measurements. The higher microwave-absorption onset temperatures may reflect the greater sensitivity of the microwave-absorption technique¹² to superconductivity in a minority higher- T_c phase in the Hg,Pb-1:2:2:3 samples. More interestingly, however, the initial microwave absorption and resistive drop may be associated with a superconducting-pair fluctuation regime above T_c in these materials. Significant order-parameter fluctuations between 133 and 145 K have also been invoked by Schilling *et al.*¹³ in Hg-1:2:2:3 in order to account for an upturn in their specific-heat data and higher-temperature resistive onsets.

Annealing the Hg,Pb-1:2:2:3 samples under reducing conditions (1% hydrogen in nitrogen) for 16 h at 300 °C decreases the sample resistivity, but has no effect on T_c . However, T_c is typically reduced to 118 K on annealing the samples in flowing oxygen at 300 °C. This suggests that the as-synthesized Hg,Pb-1:2:2:3 specimens have near-optimum hole doping levels, although some degree of underdoping is indicated by the observed increases in T_c with pressure¹⁴ and the appearance of diffuse scattering in the electron-diffraction data. The nearly single-phase Hg,Pb-1:2:1:2 samples prepared by doping the Ca sites with Y show a T_c of 115 K in SQUID magnetometer

measurements in the as-prepared condition. The T_c decreases to near 100 K on annealing in flowing oxygen, but increases to 125 K on annealing under reducing conditions at 300 °C for 16 h. This observation suggests that Y³⁺ substitution results in overdoping of the Hg,Pb-1:2:1:2 phase with holes.

The irreversibility field $H^*(T)$, which defines the boundary separating a magnetically irreversible zero-resistance state from a magnetically reversible state with a dissipative electrical resistivity, was obtained for a number of Hg,Pb-1:2:2:3 samples from the merging points of ZFC and FC magnetization data.¹⁵ The inset in Fig. 4 shows a plot of $H^*(T)$ as a function of reduced temperature for two typical Hg,Pb-1:2:2:3 samples. The linear fit (dashed line) defines the irreversibility line H_i separating the dissipative from the flux-pinned region of the magnetic phase diagram. For Hg,Pb-1:2:2:3, H_i lies at temperatures much higher than that for the three-copper-layer Bi-based cuprates⁷ and the single-copper-layer Hg and Hg,Pb compounds.^{8,9} $H^*(T)$ is 1 T at 80 K in Hg,Pb-1:2:2:3, which is substantially higher than the corresponding fields of 0.3 T and lower for the $n = 3$ phase Bi-based and the $n = 1$ phase Hg and Hg,Pb compounds. In addition, at 100 K rather low values of flux creep relative to those in the corresponding Bi- and Tl-based cuprates are observed for Hg,Pb-1:2:2:3 at fields up to 0.1 T. These encouraging initial results indicate that Hg,Pb-1:2:2:3 is likely to be an attractive candidate for high-temperature superconductor applications.

The authors would like to thank Professor K. V. Rao of the Royal Institute of Technology, Stockholm for low-field SQUID measurements on some of our samples. T. D. and A. G. R. thank the Office of Naval Research and the National Research Council respectively for their support.

¹A. Schilling, M. Cantoni, J. D. Guo, and H. R. Ott, *Nature* **363**, 56 (1993).

²C. W. Chu *et al.*, *Nature* **365**, 323 (1993).

³S. N. Putilin, E. V. Antipov, O. Chmaissem, and M. Marezio, *Nature* **362**, 226 (1993).

⁴M. Nunez-Reguerio, J.-L. Tholence, E. V. Antipov, J.-J. Capponi, and M. Marezio, *Science* **262**, 97 (1993).

⁵S. N. Putilin, E. V. Antipov, and M. Marezio, *Physica C* **212**, 266 (1993).

⁶O. Chmaissem *et al.*, *Physica C* (to be published).

⁷M. Suenaga, D. O. Welch, and R. Budhani, *Supercond. Sci. Technol.* **5**, S1 (1992).

⁸A. Umezawa *et al.*, *Nature* **364**, 129 (1993).

⁹U. Welp *et al.*, *Appl. Phys. Lett.* **63**, 693 (1993).

¹⁰Y. T. Ren *et al.* (unpublished).

¹¹M. A. Subramanian *et al.*, *Science* **242**, 249 (1988).

¹²I. I. Khairullin, A. A. Zakhidov, P. K. Khabibullaev, Z. Iqbal, and R. H. Baughman, *Synth. Met.* **33**, 243 (1989).

¹³A. Schilling, M. Cantoni, O. Jeandupeaux, J. D. Guo, and H. R. Ott (unpublished).

¹⁴C. C. Kim, D. H. Liebenberg, Z. Iqbal, and T. Datta (unpublished).

¹⁵K. A. Mueller, M. Takashige, and J. G. Bednorz, *Phys. Rev.*

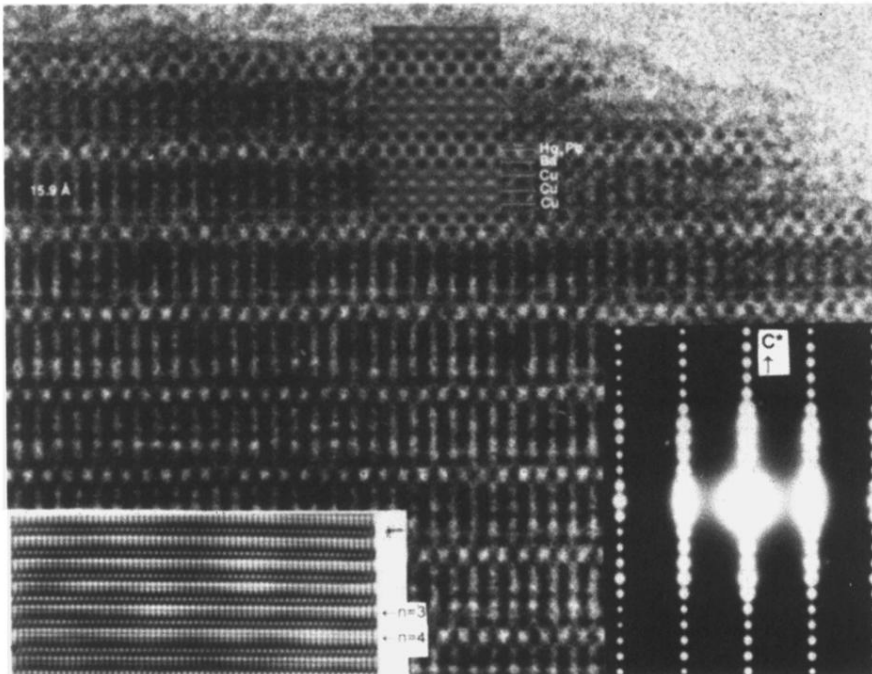


FIG. 2. [100] lattice image of a Hg,Pb-1:2:2:3 crystal. The inset at the top shows a lattice simulation. Simulation parameters are given in the text. Inset (bottom right) shows the corresponding electron-diffraction pattern, and inset (bottom left) shows a Fourier-processed (100) image.